Reconstruction Improvement of Single-Pixel Camera Based on Operator Matrix-Induced Compressive Sensing

Tao CHENG – Liuzhou[1]

ABSTRACT. A better reconstruction algorithm, a better measurement matrix, and a better denoising algorithm can all improve the signal reconstruction quality of compressive sensing. The operator matrix of a single-pixel camera has little effect on the noise in the measurement data and can improve the performance of the measurement matrix. The operator matrix can improve both the signal reconstruction quality and the reconstruction calculation speed for single-pixel camera images. Although a better reconstruction algorithm can improve the quality or speed of signal reconstruction, the operator matrix can improve the performance of the reconstruction algorithm fundamentally. The operator matrix can make reconstruction algorithms get better reconstruction ability. Moreover, the operator matrix is a universal method for improving compressive sensing.

Keywords: compressive sensing, single-pixel camera, measurement matrix, operator matrix, reconstruction algorithm.

1. Introduction

For a signal that is sparse or compressible, compressive sensing (CS) can compress the signal while it is being acquired, and can reconstruct it with high quality, at a much lower sampling frequency than the Nyquist sampling theorem requires. The mathematical model of CS is described by Eq. (1) (Cheng et al. 2016, Donoho 2006, Duarte et al. 2008, Wang et al. 2020, Zhu et al. 2012):

---

[1] Dr. Tao Cheng, School of Mechanical and Transportation Engineering, Guangxi University of Science and Technology, CN-545006 Liuzhou, Guangxi, P. R. China, e-mail: ctnp@163.com.

$$\min \| \mathbf{x} \|_0 \quad s.t. \quad \mathbf{y} = \mathbf{\Phi x}, \tag{1}$$

where $\mathbf{y}$ is the measurement data, $\mathbf{y} \in R^M$. $\mathbf{\Phi}$ denotes the measurement matrix, $\mathbf{\Phi} \in R^{M \times N}$, for which $M < N$. $\mathbf{x}$ represents the sparse signal, $\mathbf{x} \in R^N$, K is the sparsity of $\mathbf{x}$, and K<<N. $\min \| \mathbf{x} \|_0$ is the objective function, $\mathbf{y} = \mathbf{\Phi x}$ represents the constraint function, $\| \cdot \|_0$ denotes the l_0 norm, $\| \cdot \|_1$ denotes the l_2 norm, and $\| \cdot \|$ denotes the l_2 norm. Then,

$$(1 - \sigma_K) \| \mathbf{x} \|^2 \leq \| \mathbf{\Phi x} \|^2 \leq (1 + \sigma_K) \| \mathbf{x} \|^2, \tag{2}$$

where $\sigma_K \in [0,1)$.

Eq. (2) describes the restricted isometry property (RIP) of the CS. If the measurement matrix satisfies the RIP and the objective function in Eq. (1) is replaced with $\min \| \mathbf{x} \|_1$, Eq. (1) can be transformed into a convex optimization problem. Thus, the optimal solution of the sparse signal can be obtained (Candes et al. 2008, Chartrand 2007, Matcuk et al. 2020, Zhang et al. 2013).

Although different reconstruction algorithms have a great influence on the signal reconstruction effect, the performance of the measurement matrix is the decisive factor. In addition, although the RIP is perfect in theory, it is difficult to judge whether the measurement matrix satisfies the RIP; hence, its usability is poor (Duarte-Carvajalino and Sapiro 2009, Elad 2007, Tsaig and Donoho 2006).

The current main criterion for judging the performance of the measurement matrix is the maximum absolute value of the correlation coefficients between the columns (μ_{max}) of the measurement matrix (Cheng et al. 2016, Donoho 2006, Tsaig and Donoho 2006). When evaluating measurement matrices, the smaller the μ_{max}, the better the performance of the measurement matrix, implying that a better reconstruction effect can be obtained. A better measurement matrix can improve the reconstruction effectiveness of various reconstruction algorithms (Cheng et al. 2016, Duarte-Carvajalino and Sapiro 2009, Elad 2007, Zhu et al. 2012).

The remainder of this paper is organized as follows. Section 2 proposes the algorithm of the operator matrix and the method of using operator matrix in CS. Section 3 presents influence of the operator matrix on the noise of measurement data. Section 4 presents influence of the operator matrix on the performance of measurement matrix. Section 5 verifies reconstruction effectiveness of sparse signals after the operator matrix processing. SNR is higher. Section 6 verifies reconstruction time of sparse signals after the operator matrix processing. Reconstruction time is shorter. Section 7 verifies reconstruction of images after

the operator matrix processing based on the total variation minimization. Finally, Section 8 concludes the paper with a brief discussion of related issues.

2. Operator matrix

The core component of a single-pixel camera is a digital micro-mirror device (DMD). The micro-mirror on the DMD can be manipulated to indicate 0 or 1, with single-pixel cameras acquiring and compressing data through the DMD (Duarte et al. 2008, Romberg 2008, Wang et al. 2020). Although the 0-1 random matrix provides better randomness, the 0-1 circulant matrix is more conducive to programming design and operation realization. The measurement matrix of a single-pixel camera can be represented by a 0-1 random matrix or a 0-1 circulant matrix.

After completing the data acquisition process of CS, $\mathbf{A}_O$ can be obtained by performing orthogonal normalization operations on the measurement matrix $\mathbf{A}$ of a single-pixel camera. Then, the operator matrix $\mathbf{T}$ is obtained by solving $\mathbf{T} = \mathbf{A}_O \mathbf{A}^\mathrm{T} \left(\mathbf{A} \mathbf{A}^\mathrm{T} \right)^{-1}$. Here, $\mathbf{Ty} = \mathbf{TAx}$, $\mathbf{y}_\mathrm{T} = \mathbf{Ty}$, and $\mathbf{A}_O = \mathbf{TA}$. After the operator matrix processes $\mathbf{y}$ via $\mathbf{Ty} = \mathbf{TAx}$ (hereafter referred to as *the operator matrix processing*), the column irrelevance of $\mathbf{A}_O$ for the single-pixel camera becomes better than $\mathbf{A}$, and the amplification of noise in $\mathbf{y}_\mathrm{T}$ is very small. A new CS model can be obtained by replacing the constraint function in Eq. (1) with $\mathbf{Ty} = \mathbf{TAx}$, and better reconstruction effect can be obtained.

Although the reconstruction capabilities of various reconstruction algorithms used for CS are different, for the same reconstruction algorithm, the reconstruction effect depends on the balance between the performance of the measurement matrix and the strength of the noise associated with the measurement data. If the operator matrix improves the performance of the measurement matrix, the reconstruction effect of the reconstruction algorithm will be improved. Conversely, if the operator matrix increases the noise of $\mathbf{y}$, the reconstruction effect of the reconstruction algorithm is diminished, sometimes to the extent that the reconstruction process fails.

To study the effect of the operator matrix on noise and the measurement matrix in depth, we take the 0-1 random and circulant matrices as the research objects. The sizes of the 0-1 random and circulant matrices are 128×256 and 169×4096, respectively (Cheng et al. 2016, Needell and Tropp 2009, Wei and Milenkovic 2009). 128×256 0-1 random and circulant matrices are represented by rnd0-1 and rnd0-1T, and sft0-1 and sft0-1T before and after the operator matrix processing, respectively. Furthermore, 169×4096 0-1 random and circulant matrices are represented by Prnd0-1 and Prnd0-1T, and Psft0-1 and Psft0-1T before and after the operator matrix processing, respectively.

The initial row vector of the 0-1 circulant matrix is a sparse row vector. One eighth of the elements of the sparse row vector are randomly distributed ones. The elements of the upward row vector are shifted to the right by 2 places in

turn, which is the downward row vector. One eighth of the elements of the 0-1 random matrix are randomly distributed ones.

The orthogonal matching pursuit (OMP) (Abdi et al. 2019, Sreeja and Samanta 2019, Xu Ma et al. 2018) based on the l_0 norm and basis pursuit denoising (BPDN) (Chai et al. 2018, Kougioumtzoglou et al. 2020, Mahata and Hyder 2019) based on the l_1 norm are two reconstruction algorithms commonly used for CS. The OMP and BPDN are used to reconstruct the sparse signal to verify the reconstruction effect before and after the operator matrix processing.

3. Influence of the operator matrix on the noise of measurement data

The noise-to-signal ratio (NSR) of the measured data before and after the operator matrix processing are described by Eqs. (3) and (4), respectively. Fig. 1 presents the mean and standard deviation (s.d.) curves of the NSR after 500 simulations for signals at different sparsity values. Gaussian noise with a variance of 0.01 is added to the measurement data:

$$NSR = \frac{\left\| \mathbf{y}_{noi} - \mathbf{y}_{ini} \right\|}{\left\| \mathbf{y}_{ini} \right\|}, \tag{3}$$

$$NSR = \frac{\left\| \mathbf{T}\mathbf{y}_{noi} - \mathbf{T}\mathbf{y}_{ini} \right\|}{\left\| \mathbf{T}\mathbf{y}_{ini} \right\|}, \tag{4}$$

where $\mathbf{y}_{noi}$ is noisy measurement data and $\mathbf{y}_{ini}$ is noise-free measurement data.
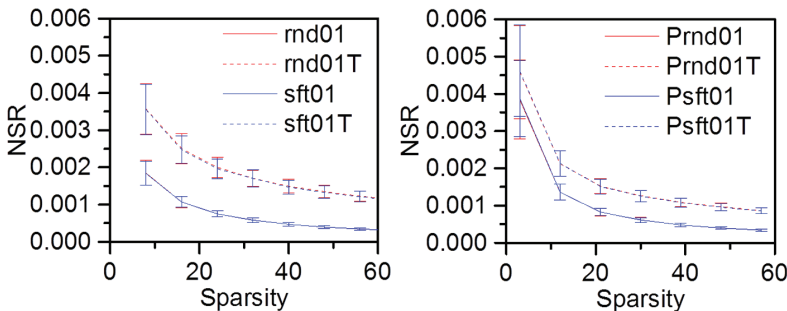

Fig. 1. *NSR vs. the sparsity of the measured data based on the 128 × 256 and 169 × 4096 0-1 random and circulant matrices before and after the operator matrix processing.*

Although the NSR curves of rnd0-1T and sft0-1T are all greater than rnd0-1 and sft0-1, the increase is small, as shown in Fig. 1. The maximum increase is only 0.0017 (i.e. 0.17%), which is almost negligible. Although the NSR curves of Prnd0-1T and Psft0-1T are all greater than Prnd0-1 and Psft0-1, the maximum increase is only 0.00074 (see Fig. 1).

4. Influence of the operator matrix on the performance of measurement matrix

The $\mu_{\max}$ of the measurement matrix is the key criterion for judging the performance of the measurement matrix (Akcakaya et al. 2011, Elad 2007). Generally, for equivalent measurement matrix types, the smaller the $\mu_{\max}$, the better the performance of the measurement matrix and the better the reconstruction effect. $\mu_{\max \mathbf{T}}$ represents the $\mu_{\max}$ after the operator matrix processing, and $\mu_d = \mu_{\max} - \mu_{\max \mathbf{T}}$. Table 1 shows the detailed $\mu_{\max}$ before and after the operator matrix processing, revealing that the $\mu_{\max}$ of the measurement matrix after the operator matrix processing decreases. They decrease by 0.181, 0.16, 0.063, and 0.053 respectively, demonstrating that the performance of all matrices has been improved after the operator matrix processing.

Table 1. *Maximum absolute value of column correlation coefficients of the 128 × 256 and 169 × 4096 0-1 random and circulant matrices before and after the operator matrix processing.*

Measurement matrix	$\mu_{\max} / \mu_{\max \mathbf{T}}$	μ_d
rnd01	0.515/0.334	0.181
sft01	0.353/0.193	0.16
Prnd01	0.537/0.474	0.063
Psft01	0.487/0.434	0.053

5. Reconstruction effectiveness before and after the operator matrix processing

Fig. 2 shows the reconstruction results of rnd0-1 and sft0-1 based on the OMP and BPDN algorithms before and after the operator matrix processing. The sparsity values of the signal are 8, 16, 24, 32, 40, 48, 56, 64, 72, and 80. The sparse signal follows the normal distribution. Gaussian noise with a variance of 0.01 was added to the measurement data and the simulation was repeated

500 times at each sparsity. After calculating the signal-to-noise (SNR) of the reconstructed results, the mean and s.d. were calculated, as shown in Fig. 2. The curves after the operator matrix processing (red curves) demonstrate a higher SNR as the sparsity increases. For very small amounts of noise growth (see Fig. 1), the improvement of measurement matrix performance (see Table 1) can improve the reconstruction ability of the reconstruction algorithm (see Fig. 2).
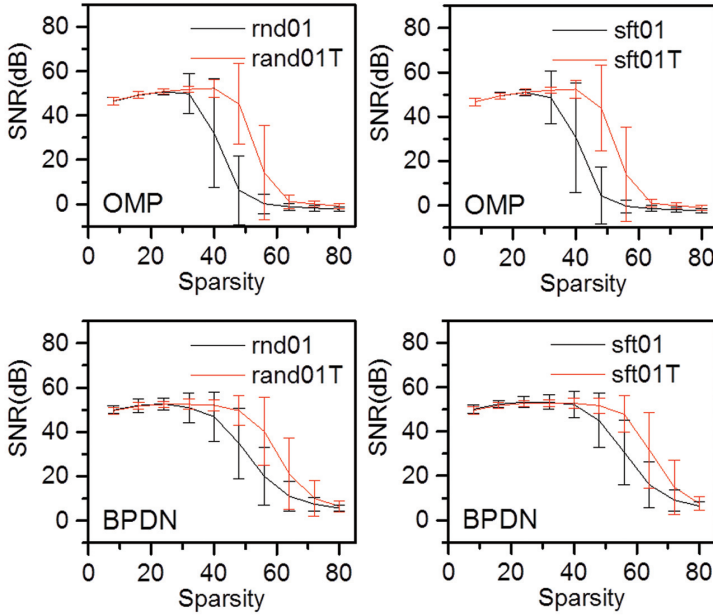

Fig. 2. *SNR vs. the sparsity of reconstruction results based on the 128 × 256 0-1 random and circulant matrices before and after the operator matrix processing by OMP and BPDN.*

Fig. 3 shows the reconstruction results of Prnd0-1, and Psft0-1 based on the OMP and BPDN algorithms before and after the operator matrix processing. The sparsity values of the signal are 3, 12, 21, 30, 39, 48, and 57. The sparse signal follows the normal distribution. Gaussian noise with a variance of 0.01 was added to the measurement data and the simulation was repeated 500 times at each signal sparsity. After calculating the SNR of the reconstructed results, the mean and s.d. were calculated (see Fig. 3). The curves of Prnd0-1T and Psft0-1T (red data) are all on the top. For very small amounts of noise growth (see Fig. 1), the improvement of measurement matrix performance (see Table 1) can improve the reconstruction ability of the reconstruction algorithm (see Fig. 3).
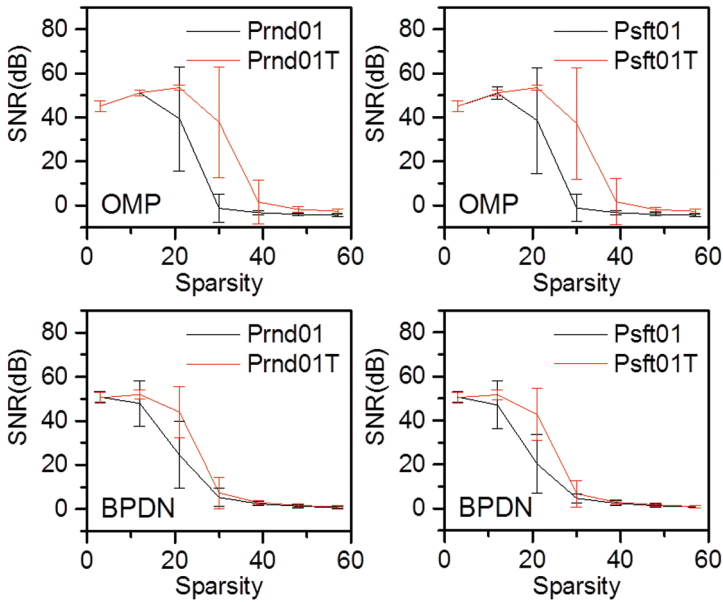
Fig. 3. *SNR vs. the sparsity of reconstruction results based on the 169 × 4096 0-1 random and circulant matrices before and after the operator matrix processing by OMP and BPDN.*

6. Reconstruction time before and after the operator matrix processing

Fig. 4 corresponds to Fig. 2. Fig. 4 represents the reconstruction time of rnd0-1 and sft0-1 based on the OMP and BPDN algorithms before and after the operator matrix processing. As the timing unit of the CPU is 1 s, in order to avoid excessive timing errors, only the total time elapsed over the course of 500 repeated simulations at the same sparsity value is counted. For the most part, the reconstruction time curves after the operator matrix processing (red curves) demonstrate shorter processing times. The true relative position of the curves of rnd0-1T and sft0-1T should be at a lower position relative to rnd0-1 and sft0-1. Because rnd0-1 and sft0-1 are sparse matrices, operations involving 0 are skipped in the Matlab processing, and no real operation time occurs. After the operator matrix processing, the sparse matrix becomes a dense matrix, and the calculation time increases greatly.
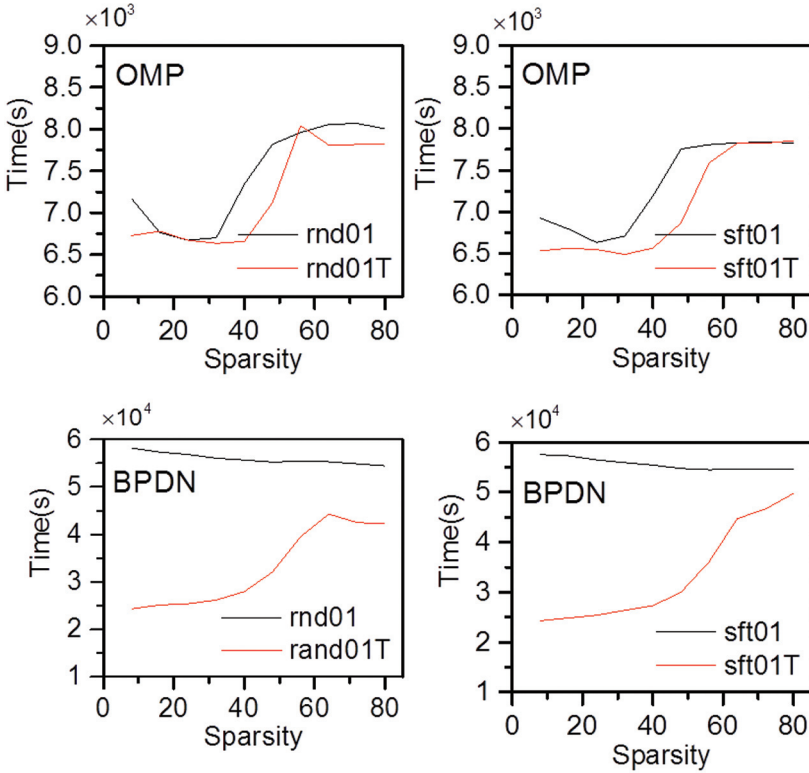
Fig. 4. *Reconstruction time vs. the sparsity of reconstruction results based on the 128 × 256 0-1 random and circulant matrices before and after the operator matrix processing by OMP and BPDN.*

Fig. 5 corresponds to Fig. 3. Fig. 5 represents the reconstruction time of Prnd0-1 and Psft0-1 based on the OMP and BPDN algorithms before and after the operator matrix processing. The true relative position of the curves of Prnd0-1T and Psft0-1T should be at a lower position relative to Prnd0-1 and Psft0-1 because Prnd0-1 and Psft0-1 are sparse matrices.
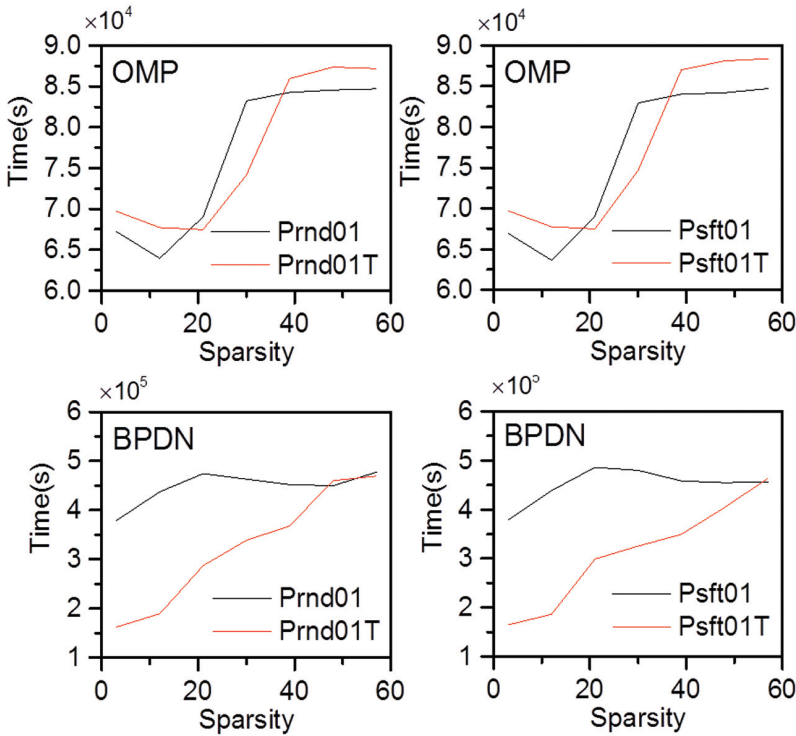
Fig. 5. *Reconstruction time vs. the sparsity of reconstruction results based on the 169 × 4096 0-1 random and circulant matrices before and after the operator matrix processing by OMP and BPDN.*

7. Reconstruction before and after the operator matrix processing based on the total variation minimization

Figs. 6 and 7 are the reconstruction results of the 0-1 random and circulant matrices, respectively, produced by the total variation minimization by the augmented Lagrangian and alternating direction algorithms (TVAL3) (Barzilai and Borwein 1988, Han and Lin 2018, Soltanlou and Latifi 2019, Wang et al. 2020, Zhang and Hager 2004) before and after the operator matrix processing. Gaussian noise with a variance of 0.01 was added to the measurement data. From left to right, the images in the first row of Figs. 6 and 7 are real images of Barbara, Boat, Cameraman, House, Mandril, Mondrian and Peppers. The image size is 64 × 64 pixels. The second row of Figs. 6 and 7 show the reconstruction results before the operator matrix processing; the third row shows the reconstruction results after the operator matrix processing, with the number pairs above the images indicating the SNR (dB) and reconstruction time (s) of the reconstructed image.
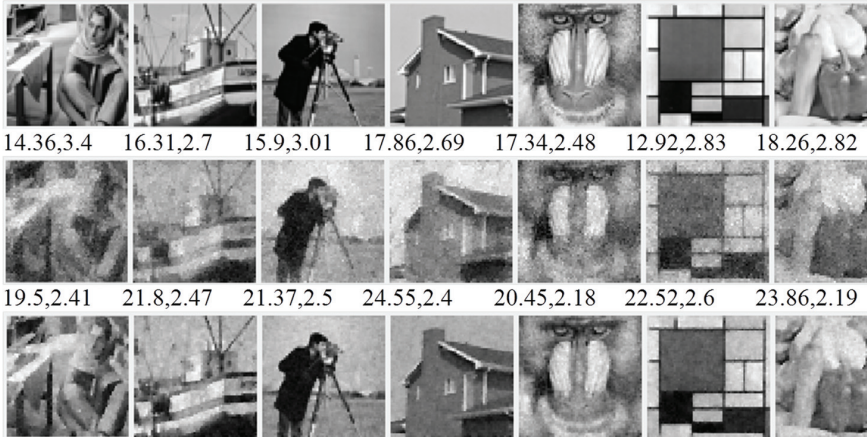
| 14.36,3.4 | 16.31,2.7 | 15.9,3.01 | 17.86,2.69 | 17.34,2.48 | 12.92,2.83 | 18.26,2.82 |
| 19.5,2.41 | 21.8,2.47 | 21.37,2.5 | 24.55,2.4 | 20.45,2.18 | 22.52,2.6 | 23.86,2.19 |

Fig. 6. *Real images vs. the reconstruction results before and after the operator matrix processing based on the 0-1 random matrix. The images in the first row are real images without noise. The second row show the reconstruction results of noisy measurement data before the operator matrix processing; the third row shows the reconstruction results of noisy measurement data after the operator matrix processing, with the number pairs above the images indicating the SNR (dB) and reconstruction time (s) of the reconstructed image.*

After the operator matrix processing for the 0-1 random matrix, the SNR increase of the 7 reconstructed images is 9.6 dB at the maximum, 3.1 dB at the minimum, and 5.87 dB on average; the reconstruction time of the 7 reconstructed images shows a maximum reduction of 0.99 s, a minimum reduction of 0.23 s, and an average reduction of 0.45 s, as shown in Fig. 6.
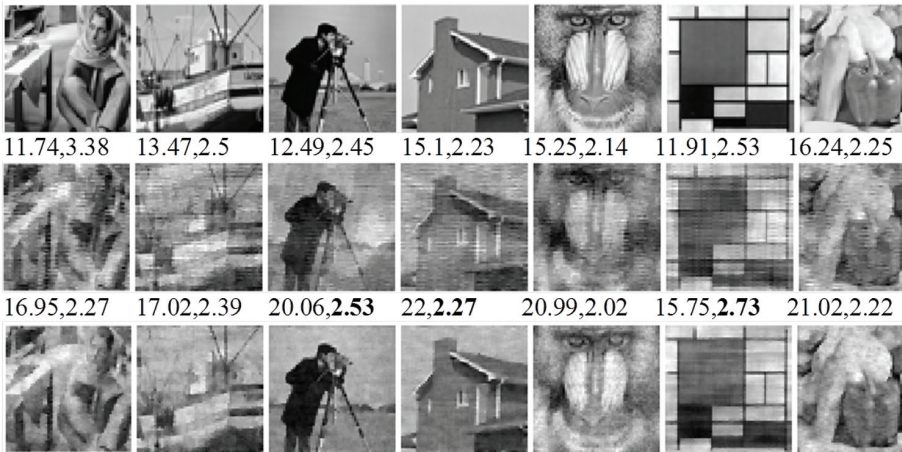

| 11.74,3.38 | 13.47,2.5 | 12.49,2.45 | 15.1,2.23 | 15.25,2.14 | 11.91,2.53 | 16.24,2.25 |
| 16.95,2.27 | 17.02,2.39 | 20.06,**2.53** | 22,**2.27** | 20.99,2.02 | 15.75,**2.73** | 21.02,2.22 |

Fig. 7. *Real images vs. the reconstruction results before and after the operator matrix processing based on the 0-1 circulant matrix.*

After the operator matrix processing for the 0-1 circulant matrix, the SNR of the 7 reconstructed images is increased by 7.57 dB at the maximum, 3.55 dB at the minimum, and 5.37 dB on average; the reconstruction time of the 7 reconstructed images shows a maximum reduction of 1.11 s, a minimum reduction of −0.2 s, and an average reduction of 0.15 s, as shown in Fig. 7.

Fig. 6 reveals that all the reconstruction times after the operator matrix processing are reduced. Almost all the reconstruction times after the operator matrix processing are reduced in Fig. 7, with the exception of the images of the Cameraman, House, and Mondrian. The true reconstruction time is less after the operator matrix processing than before the operator matrix processing. Because the 0-1 random and circulant matrices are sparse matrices, operations involving 0 are skipped in the Matlab processing, and no real operation time occurs. After the operator matrix processing, the sparse matrix becomes a dense matrix, thereby increasing the calculation time significantly.

8. Conclusion

The operator matrix of a single-pixel camera has little effect on the noise in the measurement data and can improve the performance of the measurement matrix. The operator matrix can improve the signal reconstruction quality for images captured by the single-pixel camera and speed up the reconstruction calculation speed.

After the operator matrix processing for the 0-1 random matrix, the SNR of the 7 reconstructed images (Barbara, Boat, Cameraman, House, Mandril, Mondrian and Peppers) is increased by 5.87 dB on average, and the reconstruction time of the 7 reconstructed images has an average reduction of 0.45 s. By comparison, after the operator matrix processing for the 0-1 circulant matrix, the SNR of the 7 reconstructed images is increased by 5.37 dB on average, with an average reconstruction time reduction for the 7 reconstructed images of 0.15 s.

A better reconstruction algorithm can improve the quality or speed of signal reconstruction. The operator matrix can improve the performance of the reconstruction algorithm fundamentally, thereby improving the reconstruction ability. The operator matrices is suitable for OMP based on the l_0 norm, BPDN based on the l_1 norm and TV minimum algorithm (TVAL3) in the single-pixel camera, respectively. These results demonstrate that the operator matrix is a universal CS improvement method.

References

Abdi, A., Rahmati, M., Ebadzadeh, M. M. (2019): Dictionary Learning Enhancement Framework: Learning a non-Linear Mapping Model to Enhance Discriminative Dictionary Learning Methods, Neurocomputing, Vol. 357, No. 10, 135–150.

Akcakaya, M., Jinsoo, P., Tarokh, V. (2011): A Coding Theory Approach to Noisy Compressive Sensing Using Low Density Frames, Signal Processing, IEEE Transactions on, Vol. 59, No. 11, 5369–5379.

Barzilai, J., Borwein, J. M. (1988): Two-Point Step Size Gradient Methods, IMA J. Numer. Anal., Vol. 8, No. 1, 141–148.

Candes, E. J., Wakin, M. B., Boyd, S. P. (2008): Enhancing sparsity by reweighted l1 minimization, Journal of Fourier Analysis and Applications, Vol. 14, No. 5, 877–905.

Chai, X., Zheng, X., Gan, Z., Han, D., Chen, Y. (2018): An image encryption algorithm based on chaotic system and compressive sensing, Signal Processing, Vol. 148, No. 1, 124–144.

Chartrand, R. (2007): Exact Reconstruction of Sparse Signals via Nonconvex Minimization, Signal Processing Letters, IEEE, Vol. 14, No. 10, 707–710.

Cheng, T., Chen, D., Yu, B., Niu, H. (2016): Super-resolution reconstruction of STORM images based on high-resolution recording and interpolation in compressive sensing, Biomedical Optics Express, Vol. 8, No. 5, 2445–2457.

Donoho, D. L. (2006): Compressed sensing, Information Theory, IEEE Transactions on, Vol. 52, No. 4, 1289–1306.

Duarte, M. F., Davenport, M. A., Takhar, D., Laska, J. N., Ting, S., Kelly, K. F., Baraniuk, R. G. (2008): Single-Pixel Imaging via Compressive Sampling, Signal Processing Magazine, IEEE, Vol. 25, No. 2, 83–91.

Duarte-Carvajalino, J. M., Sapiro, G. (2009): Learning to Sense Sparse Signals: Simultaneous Sensing Matrix and Sparsifying Dictionary Optimization, Image Processing, IEEE Transactions on, Vol. 18, No. 7, 1395–1408.

Elad, M. (2007): Optimized Projections for Compressed Sensing, Signal Processing, IEEE Transactions on, Vol. 55, No. 12, 5695–5702.

Han, G., Lin, B. (2018): Optimal sampling and reconstruction of undersampled atomic force microscope images using compressive sensing, Ultramicroscopy, Vol. 189, No. 6, 85–94.

Kougioumtzoglou, I. A., Petromichelakis, I., Psaros, A. F. (2020): Sparse representations and compressive sampling approaches in engineering mechanics: A review of theoretical concepts and diverse applications, Probabilistic Engineering Mechanics, Vol. 61, No. 7, 1–20.

Mahata, K., Hyder, M. M. (2019): Sparse deconvolution via off-grid T.V minimization, Signal Processing, Vol. 170, No. 170, 1–15.

Matcuk, G. R., Gross, J. S., Fritz, J. (2020): Compressed Sensing MRI: Technique and Clinical Applications, Advances in Clinical Radiology, Vol. 2, No. 9, 257–271.

Needell, D., Tropp, J. A. (2009): CoSaMP: Iterative signal recovery from incomplete and inaccurate samples, Applied and Computational Harmonic Analysis, Vol. 26, No. 3, 301–321.

Romberg, J. (2008): Imaging via Compressive Sampling, Signal Processing Magazine IEEE, Vol. 25, No. 2, 14–20.

Soltanlou, K., Latifi, H. (2019): Compressive ghost imaging in the presence of environmental noise, Optics Communications, Vol. 436, No. 4, 113–120.

Sreeja, S. R., Samanta, D. (2019): Classification of multiclass motor imagery EEG signal using sparsity approach, Neurocomputing, Vol. 368, No. 27, 133–145.

Tsaig, Y., Donoho, D. L. (2006): Extensions of compressed sensing, Signal Processing, Vol. 86, No. 3, 549–571.

Wang, P., Liang, J., Wang, L. V. (2020): Single-shot ultrafast imaging attaining 70 trillion frames per second, Nature Communications, Vol. 11, No. 5, 1–9.

Wei, D., Milenkovic, O. (2009): Subspace Pursuit for Compressive Sensing Signal Reconstruction, Information Theory, IEEE Transactions on, Vol. 55, No. 5, 2230–2249.

Xu Ma, F. Y., Sicong, L., Jian, S. (2018): Channel estimation for wideband underwater visible light communication: a compressive sensing perspective, Opt. Express, Vol. 26, No. 1, 311–321.

Zhang, H., Hager, W. W. (2004): A nonmonotone line search technique and its application to unconstrained optimization, SIAM Journal on Optimization, Vol. 14, No. 4, 1043–1056.

Zhang, Z., Shi, Y., Ding, W., Yin, B. (2013): MR images reconstruction based on TVWL2–L1 model, Journal of Visual Communication and Image Representation, Vol. 24, No. 2, 187–195.

Zhu, L., Zhang, W., Elnatan, D., Huang, B. (2012): Faster STORM using compressed sensing, Nature methods, Vol. 9, No. 7, 721–723.

Poboljšanje rekonstrukcije kamere s jednim pikselom na temelju kompresivnog istraživanja induciranog matricom operatora

SAŽETAK. Bolji algoritam rekonstrukcije, bolja matrica mjerenja te bolji algoritam za smanjenje šuma mogu poboljšati kvalitetu rekonstrukcije signala. Matrica operatora kamere s jednim pikselom ima mali učinak na šum u mjernim podacima te može poboljšati performanse matrice mjerenja. Matrica operatora može poboljšati i kvalitetu rekonstrukcije signala kao i brzinu izračuna rekonstrukcije signala za snimke kamerom s jednim pikselom. Iako bolji algoritam rekonstrukcije može poboljšati kvalitetu ili brzinu rekonstrukcije signala, matrica operatora može u osnovi poboljšati performanse algoritma rekonstrukcije. Matrica operatora može utjecati na to da algoritmi rekonstrukcije dobiju bolju sposobnost rekonstrukcije. Osim toga, matrica operatora je univerzalna metoda za poboljšanje kompresivnog istraživanja.

Ključne riječi: kompresivno istraživanje, kamera s jednim pikselom, matrica mjerenja, matrica operatora, algoritam rekonstrukcije.